Electronic Supplementary Information (ESI)

Cu_xS nanoparticle@carbon nanorod composites prepared from metal-organic framework as efficient electrode catalysts in quantum dot sensitized solar cells

Yuan Wang[†a], Mingshui Yao[†b], Lianjing Zhao[a], Wei Wang[a], Weinan Xue[a], Yan Li*[a]

[a]Key Laboratory for Advanced Materials, Shanghai Key Laboratory of Functional Materials Chemistry, School of Chemistry and Molecular Engineering, East China University of Science and Technology, Shanghai 200237, China

[b]State Key Laboratory of Structural Chemistry, Fujian Institute of Research on the Structure of Matter, Chinese Academy of Sciences(CAS), Fuzhou, Fujian, 350002 P. R. China

[†]These authors contributed equally to this work

*E-mails: yli@ecust.edu.cn

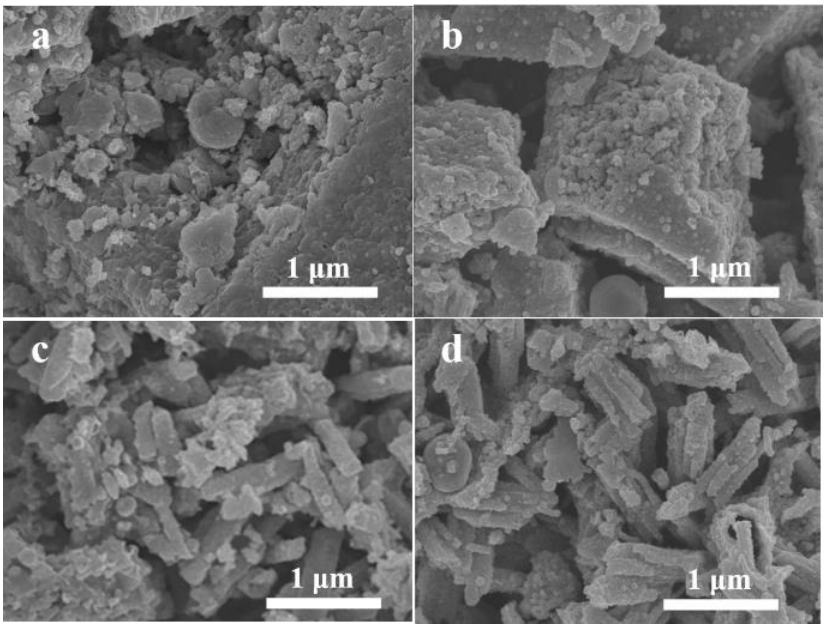

Fig. S1 SEM images of internal of (a) Cu@C-800, (b) Cu@C-900, (c) Cu@C-1000, (d) Cu@C-1100.

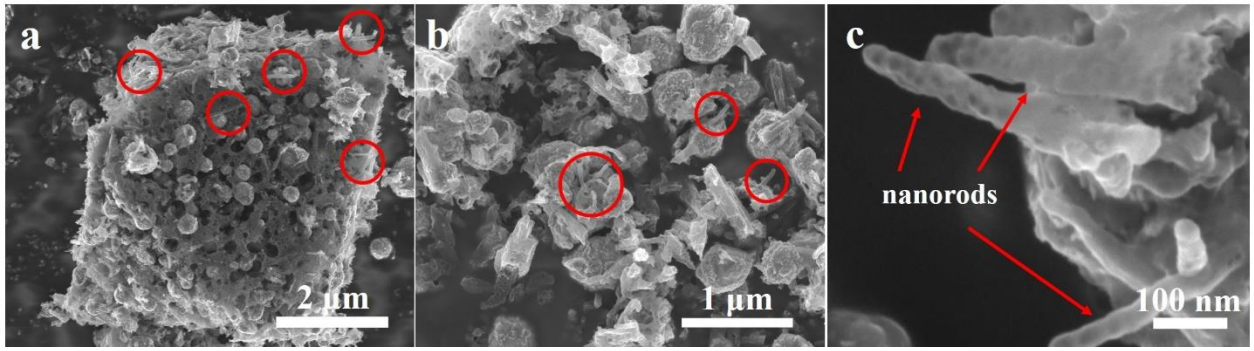

Fig. S2 SEM images of (a) octahedral geometry and (b) internal of Cu@C-950 (inside red circles are half-baked carbon nanorods). (c) Enlarged view of nanorods on the surface of Cu@C-950.

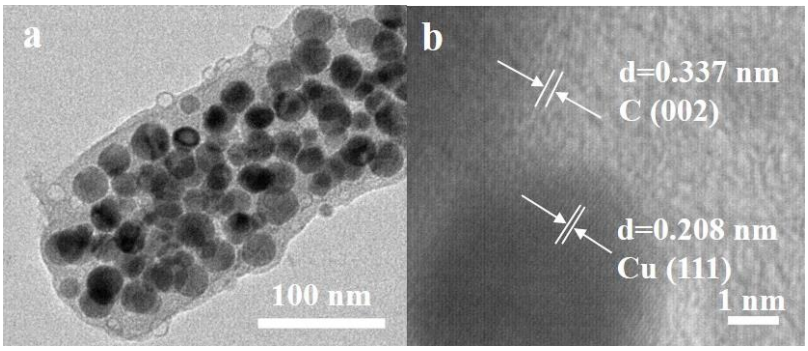

Fig. S3 TEM images of (a) Cu@C-1100, (b) High-resolution TEM of Cu@C-1100 with Cu nanoparticles encased in the graphitic carbon (insert: lattice fringes of the crystalline Cu NPs of Cu@C-1100).

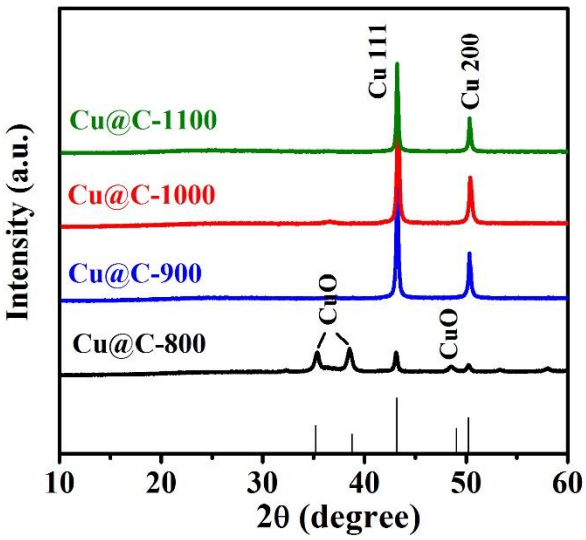

Fig. S4 Powder XRD patterns of Cu@C-*x* (Cubic Cu: 00-001-1241, Cubic CuO: 00-002-1041)

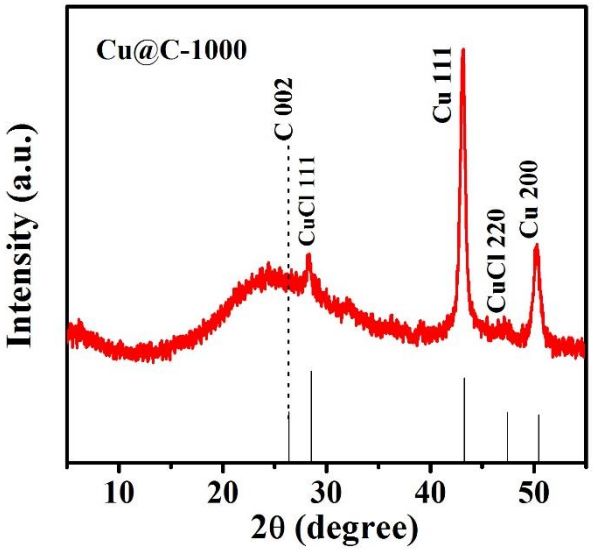

Fig. S5 Powder XRD patterns of the Cu@C-1000 sample treated by aqua regia (C: 41-1487, CuCl: 06-0344).

The presence of CuCl diffraction peaks at $2\theta = 28.5^{o}$ and 47.4^{o} are attributed to the chemical reaction between aqua regia and Cu NPs.

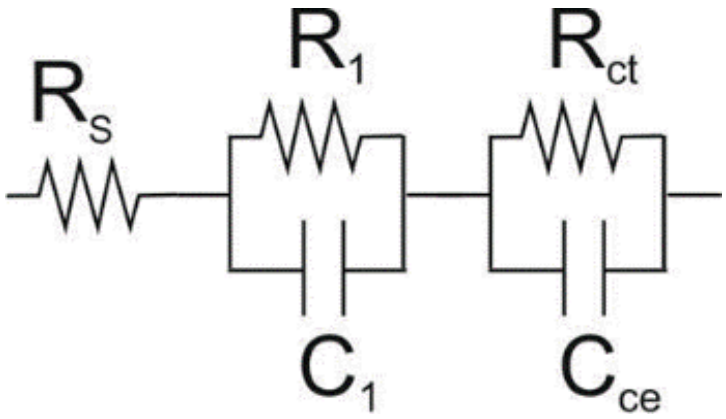

Fig. S6 Simulation circuit used for analysing the EIS data for symmetric dummy cells. R_s accounts for substrate resistance, R_1 and C_1, associated to high frequency arc, for charge transfer resistance and contact capacitance at interface between substrate and carbon electrode, R_{ct} and C_{ce}, associated to low frequency arc, for charge transfer resistance and electrode capacitance at CE/electrolyte interface.

Table S1 Parameters from EIS measurements of different CEs.

Electrodes	R_s (Ω cm^2)	$2R_1$ (Ω cm^2)	$2C_1$ (mF/cm^2)	$2R_{ct}$ (Ω cm^2)	$2C_{ce}$ (F/cm^2)
Cu@C-800	8.257	0.864	24.358	1.478	0.264
Cu@C-900	8.325	0.660	14.362	1.382	0.373
Cu@C-1000	8.280	0.325	0.026	0.353	0.069
Cu@C-1100	8.295	0.244	0.503	0.702	0.058
Cu_2S	8.456	0.583	3.592	1.328	0.288

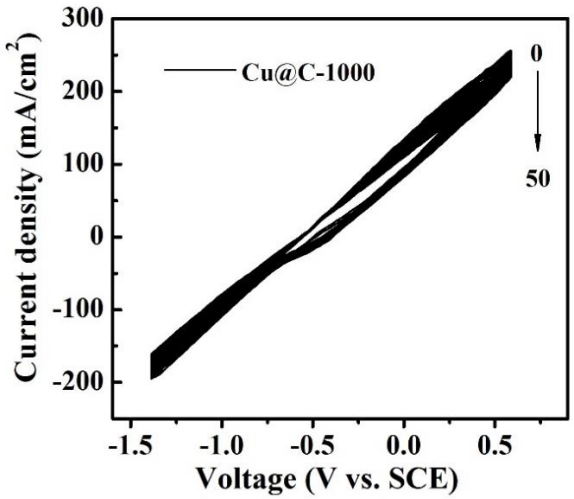

Fig. S7 Consecutive CV measurement for 50 cycles about Cu@C-1000/FTO CEs at a scan rate of 100 mV·s^{-1} in the media of S_n^{2-}/S^{2-} redox electrolyte.

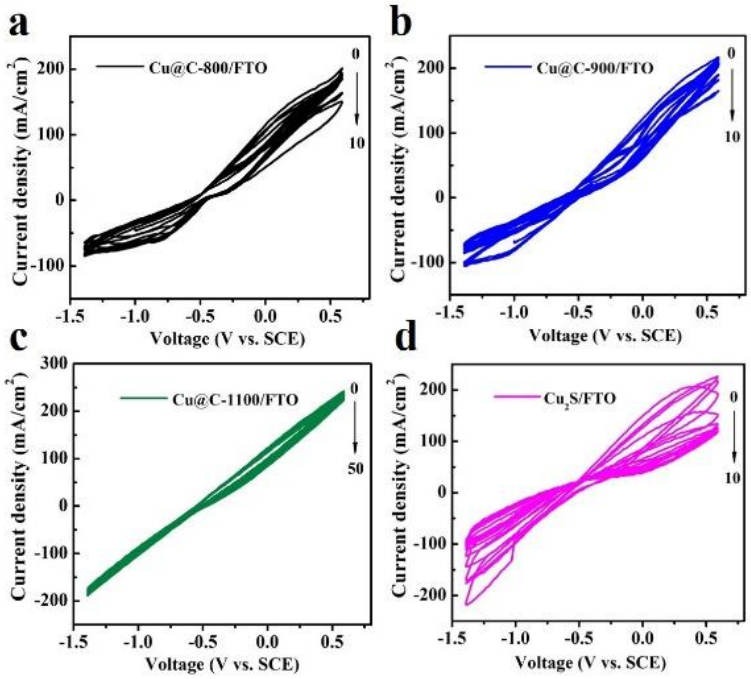

Fig. S8 Electrochemical stability of different CEs. Consecutive CV measurement for 10 cycles of (a) Cu@C-800/FTO, (b) Cu@C-900/FTO, 50 cycles of (c) Cu@C-1100/FTO, and 10 cycles of (d) Cu_2S/FTO, and at a scan rate of 100 $mV \cdot s^{-1}$ in the media of S_n^{2-}/S^{2-} redox electrolyte, respectively.

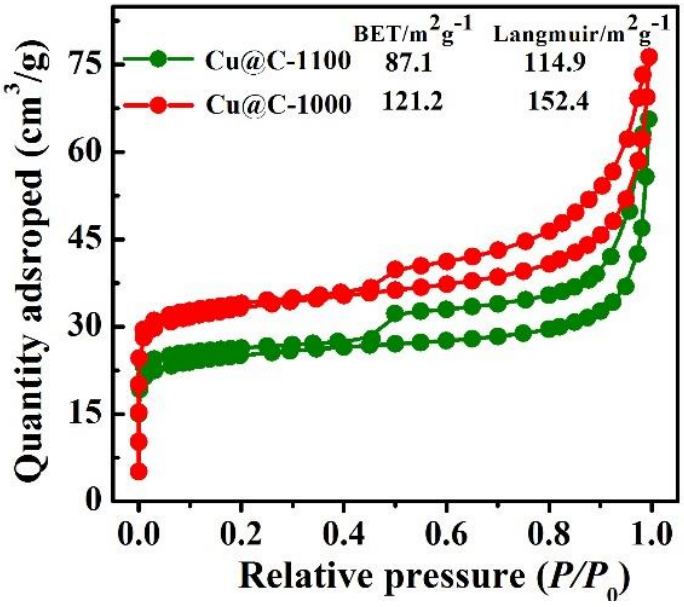

Fig. S9 Nitrogen adsorption isotherms measured at 77 K of Cu@C-1000 and Cu@C-1100 (insert: pore parameters of Cu@C-1000 and Cu@C-1100).

Table S2 Pore parameters of Cu@C-*x* samples.

Samples	S_{BET} (m^2/g)
Cu@C-800	130.88
Cu@C-800	114.85
Cu@C-800	99.59
Cu@C-800	121.69
Cu@C-800	87.13

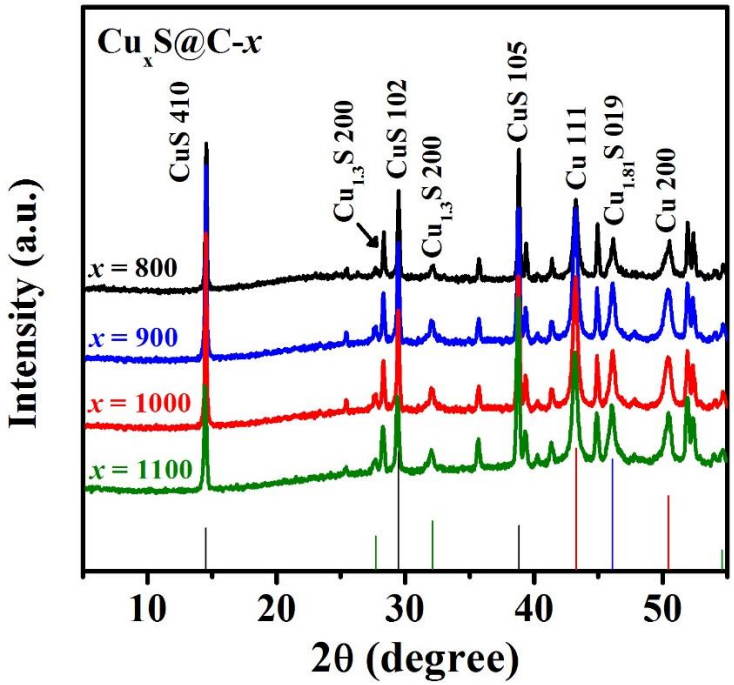

Fig. S10 Powder XRD patterns of obtained Cu_xS@C-*x*. (JCPDS information: red line is cubic Cu 04-0836, green line is Cubic $Cu_{1.3}S$ 24-0061, blue line is cubic $Cu_{1.81}S$ 41-0959, black line is cubic CuS 06-0464).

Table S3 Inductively coupled plasma atomic emission spectrometry (ICP-AES) results for Cu contents in the aqueous solution soaked by Cu_xS@C-*x* samples.

Samples	Cu (mg/L)
Cu_xS@C-800/FTO	2.77
Cu_xS@C-900/FTO	2.58
Cu_xS@C-1000/FTO	0.74
Cu_xS@C-1100/FTO	0.72
Cu_2S/FTO	1.10